Subpixel Image Registration by Estimating the Polyphase Decomposition of Cross Power Spectrum

H. Shekarforoush   M. Berthod   J. Zerubia

INRIA - 2004 route des Lucioles
B.P. 93, 06902 Sophia Antipolis
FRANCE
email: hshekar@sophia.inria.fr
Fax: (+33) 93 65 76 43

Abstract

A method of registering images at subpixel accuracy has been proposed, which does not resort to interpolation. The method is based on the phase correlation method and is remarkably robust to correlated noise and uniform variations of luminance. We have shown that the cross power spectrum of two images, containing subpixel shifts, is a polyphase decomposition of a Dirac delta function. By estimating the sum of polyphase components one can then determine subpixel shifts along each axis.

1 Introduction

Image registration is an essential requirement for several image analysis issues such as temporal change detection, stereo matching, motion analysis and many other image sequence analysis. Many of these problems require only registration at pixel level [5] [6], while others [3] [7] [8] [12] [13] [14] depend on the scene registration at subpixel accuracy.

The most commonly used approaches for subpixel registration require interpolating at some stage. Amongst this class of algorithms we can notably mention: correlation interpolation [4] [15], intensity interpolation[15], phase correlation interpolation [10] [15] and the geometric methods [2]. It is obvious that the accuracy of these methods depends highly on the quality of the interpolation algorithm.

Methods that do not use interpolation for achieving subpixel accuracy, have been more scarce in the litterature. Most of these methods, rely on the differential properties of image frames [6] [7] [15]. There are, however, several difficulties associated with differential methods: they can only be used when the interframe displacements are very small compared to intensity variations, image gradient is only approximated using finite difference methods and finally these methods exhibit high sensitivity to noise.

Another class of algorithms are those that are based on optimisation [9] [16]. These algorithms implicitly use interpolation by allowing somewhat direct passage from discrete to the continuous domain

In the following section, we will briefly describe the phase correlation method. We then present the method proposed herein, followed by some error analysis. And finally experimental results are provided with some concluding remarks at the end.

2 The Phase Correlation Method

The idea behind this method [10] is quite simple and is based on the Fourier shift theorem [11] and the fact that for two images with some degree of congruence, the signal power in their cross power spectrum is mostly concentrated in a coherent peak located at the point of registration while the noise power is distributed randomly in some incoherent peaks.

Let $f_1(x, y)$ and $f_2(x, y)$ be two functions defined on $\mathbb{R}^2$ and:

$$\mathfrak{F}\{f_1(x, y)\} = F_1(\omega_x, \omega_y)$$
$$\mathfrak{F}\{f_2(x, y)\} = F_2(\omega_x, \omega_y)$$

where $\mathfrak{F}$ denotes the Fourier transform.

Let also: $f_2(x, y) = f_1(x + x_0, y + y_0)$ (1)

Then according to Fourier shift theorem:

$$F_2(\omega_x, \omega_y) = F_1(\omega_x, \omega_y)\, e^{j(\omega_x x_0 + \omega_y y_0)} \qquad (2)$$

Or equivalently:

$$\frac{F_2(\omega_x, \omega_y)\, F_1^*(\omega_x, \omega_y)}{\mid F_2(\omega_x, \omega_y)\, F_1^*(\omega_x, \omega_y) \mid} = e^{j(\omega_x x_0 + \omega_y y_0)} \qquad (3)$$

where $*$ denotes the complex conjugate and the left hand side is refered to as the cross power spectrum of the two functions (actually their normalized cross

power spectrum).

It is now a simple matter to determine x_0 and y_0, since the inverse Fourier transform of the right hand side is a Dirac delta function centered at (x_0, y_0):

$$\mathfrak{F}^{-1}\left(\frac{F_2(\omega_x, \omega_y)\, F_1^*(\omega_x, \omega_y)}{\mid F_2(\omega_x, \omega_y)\, F_1^*(\omega_x, \omega_y) \mid} \right) = \mathfrak{F}^{-1}\left(e^{j(\omega_x x_0 + \omega_y y_0)} \right)$$

$$= \delta(x_0, y_0) \qquad (4)$$

In practice, when dealing with images, f_1 and f_2 are only specified in finite size discretized arrays. Replacing the Fourier transform by its finite size discrete version while assuming periodic extension of images and also replacing the Dirac delta function by the unit impulse, it has been shown [10] that the above results still hold, despite the periodicity assumption and the fact that truncated discrete Fourier coefficients are employed.

This method has a remarkable robustness to correlated noise and uniform time varying illumination, making it more appropriate in most practical applications compared to classical cross correlation method. Besides, using the convolution theorem, it can be easily shown that the method can handle blurred images, since the blurring kernel would become a multiplicative factor in the spectral domain and would vanish in equation (4).

However, in the discrete case equation (2) is only valid, if the shift vector (x_0, y_0) is of integer values. Therefore, when applied to discrete images, the method would fail to detect non-integer subpixel shifts. The only approach, proposed in the literature, for adapting the method for subpixel estimation is the use of interpolation methods [10] [15].

A second important issue to point out about the phase correlation method is that, in shifts of pixel order the inverse Fourier transform of the cross power spectrum always contains a single coherent peak, at the point of registration, corresponding to signal power, and some incoherent peaks which can be assumed to be distributed normally over a mean value of zero [10]. The amplitude of the coherent peak is a direct measure of the degree of congruence between the two images. More precisely, the power in the coherent peak corresponds to the percentage of overlapping areas, while the power in incoherent peaks correspond to the percentage of non-overlapping areas.

3 Subpixel Registration

Motivated by searching for a method which embodies advantages of the phase correlation method described above, we will investigate, herein, the possibility of extracting subpixel (ie. non-integer) displacements between two images using their cross power spectrum. For this purpose, we will assume that, at some stage, two images with integer value displacements between them, have been downsampled, reducing the correspondence between them to subpixel

values. In the following section, we will, therefore, examine the cross power spectrum of two downsampled images. Downsampling, which can be seen as a polyphase decomposition in the spectral domain is discussed in [1] [17] for multidimensional cases.

3.1 Preliminaries

Consider two images, $f(x, y)$ and $f(x + x_0, y + y_0)$, where the displacement vector (x_0, y_0) is an integer valued vector. Let also $\mathfrak{F}$ $(f(x, y)) = F(\omega_x, \omega_y)$ and $\mathfrak{F}$ $(f(x + x_0, y + y_0)) = F(\omega_x, \omega_y) exp(j(\omega_x x_0 + \omega_y y_0))$ denote their discrete Fourier transforms. Then the corresponding discrete Fourier transforms after downsampling the images by factors of M and N along x and y axes respectively, will be given by (see [1] [17]):

$$\Phi_1(\omega_x', \omega_y') = \frac{1}{MN} \sum_{m=0}^{M-1} \sum_{n=0}^{N-1} F(\omega_x', \omega_y') \qquad (5)$$

$$\Phi_2(\omega_x', \omega_y') = \frac{1}{MN} \sum_{m=0}^{M-1} \sum_{n=0}^{N-1} F(\omega_x', \omega_y') exp(j(\omega_x' x_0 + \omega_y' y_0))$$

$$\qquad (6)$$

where $\omega_x' = \frac{\omega_x}{M} + \frac{2\pi m}{M}$, $\omega_y' = \frac{\omega_y}{N} + \frac{2\pi n}{N}$ and Φ_1 and Φ_2 are the downsampled spectra.

Therefore, the cross power spectrum of the downsampled images will be given by:

$$C(\omega_x', \omega_y') = \frac{\frac{1}{MN}\sum_{m=0}^{M-1}\sum_{n=0}^{N-1} F(\omega_x', \omega_y') exp(j(\omega_x' x_0 + \omega_y' y_0))}{\frac{1}{MN}\sum_{m=0}^{M-1}\sum_{n=0}^{N-1} F(\omega_x', \omega_y')}$$

$$= \sum_{m=0}^{M-1}\sum_{n=0}^{N-1} H_{mn}(\omega_x', \omega_y') exp(j(\omega_x' x_0 + \omega_y' y_0)) \qquad (7)$$

where $H_{mn}(\omega_x', \omega_y') = \frac{F(\omega_x', \omega_y')}{\sum_{m=0}^{M-1}\sum_{n=0}^{N-1} F(\omega_x', \omega_y')}$ $\qquad (8)$

Comparing the above results with those in chap. 2 of [17] on the polyphase transform of signals, we notice that the cross power spectrum of two downsampled images is, merely, a polyphase decomposition of a filtered Dirac delta function. Here, the filters $H_{mn}(\omega_x', \omega_y')$ can be easily identified by substituting back ω_x' and ω_y' and rearranging equation (8):

$$H_{mn}(\omega_x', \omega_y')\sum_{m=0}^{M-1}\sum_{n=0}^{N-1} F(\frac{\omega_x}{M} + \frac{2\pi m}{M}, \frac{\omega_y}{N} + \frac{2\pi n}{N})$$

$$= F(\frac{\omega_x}{M} + \frac{2\pi k}{M}, \frac{\omega_y}{N} + \frac{2\pi l}{N}) \qquad (9)$$

where $k \in [0 \ldots M - 1]$ and $l \in [0 \ldots N - 1]$.

It is obvious from this last equation that:

$$H_{mn}(\omega_x', \omega_y') = \begin{cases} 1 & \text{if } (m = k \text{ AND } n = l) \\ 0 & \text{otherwise} \end{cases} \qquad (10)$$

To identify the bandwidth of each filter H_{mn}, recall that both ω_x and ω_y are in $[0, 2\pi]$, and hence :
$\omega_x' \in [\frac{2\pi m}{M}, \frac{\pi}{M} + \frac{2\pi m}{M}]$ and $\omega_y' \in [\frac{2\pi n}{N}, \frac{2\pi}{N} + \frac{2\pi n}{N}]$.

In fact, it is well known [17] that filtering a down-sampled image using a bank of filters is equivalent to filtering the upsampled version by a single upsampled filter and then downsampling the output. This can also be easily verified, in our setup, where the cross power spectrum is a Dirac delta function filtered by a single upsampled filter followed by downsampling the output. Figure 1 shows the spatial domain and the frequency domain response of such a filter (a 2D sinc function in the spatial domain).
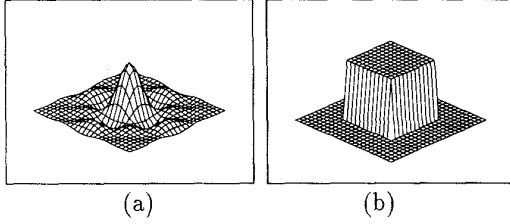

Figure 1: (a) spatial response of overal filter, (b) frequency response

The main result of this section can, therefore, be summarized as follows:

In general the cross power spectrum of two images is a Dirac delta function. However in the case of down-sampled images we have shown that the cross power spectrum is a filtered Dirac delta function which has then been downsampled. The filter has a 2D sinc spatial response.

3.2 Estimating the Sum of Polyphase Components

Equation (7), ideally, provides the cross power spectrum of two downsampled images. We should, however, point out that the relation holds under period-icity assumption and hence, for two real images with subpixel shifts, since the images are only observed in one period, we should expect some additive noise due to non-overlapped regions. This additive noise will be assumed to be distributed normaly over a mean value of zero, as was the case for integer displacements [10]. In other words, we will assume to have:

$$\mathfrak{F}^{-1}\left(C_\eta(\omega'_x, \omega'_y)\right) = \mathfrak{F}^{-1}\left(C(\omega'_x, \omega'_y)\right) + \eta(x, y) \quad (11)$$

where $\eta(x, y)$ is a zero mean Gaussian noise and C_η is the cross power spectrum with noise.

In general, the problem could be easily solved if we could estimate the polyphase components of the cross power spectrum, in which case the problem would reduce to a linear matrix equation, as described in [17]. However, using equation (7), we can, at best, expect to estimate the sum of the polyphase components rather than each individual one. We will, however, see that this estimate will be sufficient for our purpose.

From the results obtained in the previous section and making use of the Fourier shift theorem, we get:

$$\mathfrak{F}^{-1}(C(\omega'_x, \omega'_y)) = \frac{sin(\pi(Mx + x_0))}{\pi(Mx + x_0)} \frac{sin(\pi(Ny + y_0))}{\pi(Ny + y_0)} \quad (12)$$

Therefore, if $c_\eta(x, y) = \mathfrak{F}^{-1}\left(C_\eta(\omega'_x, \omega'_y)\right)$, then:

$$c_\eta(x, y) = \frac{sin(\pi(Mx + x_0))}{\pi(Mx + x_0)} \frac{sin(\pi(Ny + y_0))}{\pi(Ny + y_0)} + \eta(x, y) \quad (13)$$

At the first glance, this last equation seems to be an ideal setup for using a Maximum Likelyhood estimator for extracting (x_0, y_0). However, decoupling the unknown variables proves to be not so straightforward. Therefore, we will suggest a different approach based on estimating an upper bound for the noise variance and a lower bound for the signal variance which, in turn, will allow us to separate the noise process by setting a threshold value.

Before, proceeding with variance estimations, we shall recall that, since the cross power spectrum has been normalized, we will be only interested in the normalized values of the variances taking values in the interval $[0, 1]$. Now, consider the case when the image dimensions are $X \times Y$. Then, since the non-overlapped regions are of subpixel width (see Figure 2) and also since the noise power is given by the percentage of non-overlapped area in each image, we can estimate the following upper bound for the noise variance:

$$\sigma_\eta^2 < \frac{(X + Y)^2}{(XY)^2} \quad (14)$$

Similarly, a lower bound for the total signal power would be:

$$\sigma_s^2 \geq \frac{(XY - (X + Y))^2}{(XY)^2} \quad (15)$$

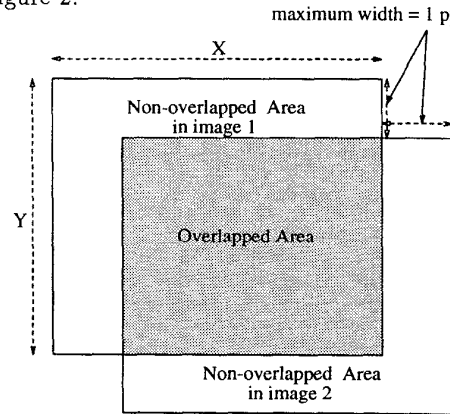These estimations are based on the schematic diagram in Figure 2:

Figure 2: Overlay of two images

Therefore, the minimum signal to noise ratio can be found by:

$$SNR = 10 \, log\left(\frac{\sigma_s^2}{\sigma_\eta^2}\right) > 10 \, log\left(\frac{(XY-(X+Y))^2}{(X+Y)^2}\right) \quad (16)$$

It is obvious that for subpixel shifts the SNR is very large. Therefore, the choice of a noise threshold value T_η is not a great concern, although in the next section we will provide a rigorous method of choosing it. Thus, the signal is simply detected by using:

$$c(x,y) = c_\eta(x,y) \quad \text{if} \quad c_\eta(x,y) > T_\eta \quad (17)$$

Once $c(x,y)$ has been estimated, (x_0, y_0) can be calculated by straight application of equation (12) to a set of points. Note, however, that results will be more reliable if equation (12) is applied to points where the signal power is mostly concentrated (see next section). In fact for two images with displacements at subpixel order, the signal energy is expected to be mostly concentrated between pixels in the area $[-1,1] \times [-1,1]$ (negative pixel locations follow the periodicity assumption, eg. pixel $(-1,0)$ corresponds to $(X-1,0)$).

We will illustrate the method using an example:

Consider the situation where the signal power is mostly concentrated at pixels $(0,0)$, $(1,0)$ and $(0,1)$. Then applying equation (12) to the first two points will yield:

$$\frac{sin(\pi x_0)}{\pi x_0} \frac{sin(\pi y_0)}{\pi y_0} = c(0,0) \quad (18)$$

$$\frac{sin(\pi(M+x_0))}{\pi(M+x_0)} \frac{sin(\pi y_0)}{\pi y_0} = c(1,0) \quad (19)$$

dividing both sides and rearranging, we get:

$$\frac{sin(\pi(M+x_0))}{\pi(M+x_0)} = \frac{c(1,0)}{c(0,0)} \frac{sin(\pi x_0)}{\pi x_0} \quad (20)$$

Or:

$$\frac{\pm sin(\pi x_0)}{(M+x_0)} = \frac{c(1,0)}{c(0,0)} \frac{sin(\pi x_0)}{x_0} \quad (21)$$

And after simplifying we obtain:

$$\frac{x_0}{M} = \frac{c(1,0)}{\pm c(0,0) - c(1,0)} \quad (22)$$

where $\Delta x = \frac{x_0}{M}$ is the subpixel displacement along the x-axis. Note that, no knowledge of the downsampling rate M is required. Note also that two solutions will be obtained. This ambiguity is due to the isotropic form of $c(x,y)$ and, in fact, only one of these solutions (ie. the right solution) is in the interval $[-1,1]$. Similarly, we can find $\Delta y = \frac{y_0}{N}$ by using, for instance, $c(0,0)$ and $c(0,1)$.

3.3 Error Analysis

For the error analysis, we can use a method similar to the one adopted by [10]. The only difference here, is that the signal power is not concentrated in a single coherent peak, but due to the polyphase decomposition of the cross power spectrum, it is distributed in a set of coherent peaks mostly adjacent to each other. In fact this is nicely described by equations (7) and (12) above.

Since we have assumed a normal distribution of the noise around a mean value of zero, the probability that the noise value exceeds T_η will be given by:

$$\begin{aligned} \mathcal{P}_{T_\eta}(\eta) &= \frac{1}{\sqrt{2\pi}\sigma_\eta} \int_{T_\eta}^{\infty} exp\left(-\frac{\eta^2}{2\sigma_\eta^2}\right) d\eta \\ &= \frac{1}{\sqrt{2\pi}\sigma_\eta} \int_{T_\eta}^{1} exp\left(-\frac{\eta^2}{2\sigma_\eta^2}\right) d\eta \quad (23) \end{aligned}$$

The last equality is due to normalization of the cross power spectrum between zero and one.

On the other hand, in this interval, we can write the following inequality:

$$\frac{1}{\sqrt{2\pi}\sigma_\eta} \int_{T_\eta}^{1} exp\left(-\frac{\eta^2}{2\sigma_\eta^2}\right) d\eta > \frac{1}{\sqrt{2\pi}\sigma_\eta} \int_{T_\eta}^{1} \eta \, exp\left(-\frac{\eta^2}{2\sigma_\eta^2}\right) d\eta \quad (24)$$

This inequality follows from the fact that, in the interval where the integrals have been taken, the integrand on the left hand side is always larger than the integrand on the right hand side. Therefore substituting equation (23) into (24) and computing the integral on the right hand side, we will obtain:

$$\mathcal{P}_{T_\eta}(\eta) > \frac{\sigma_\eta}{\sqrt{2\pi}} \left(exp\left(\frac{-T^2}{2\sigma_\eta^2}\right) - exp\left(\frac{-1}{2\sigma_\eta^2}\right)\right) \quad (25)$$

And after rearranging and simplifying, we will have:

$$T_\eta^2 > -2\sigma_\eta^2 \, ln\left(\frac{\sqrt{2\pi}\mathcal{P}_{T_\eta}(\eta)}{\sigma_\eta} + exp\left(\frac{-1}{2\sigma_\eta^2}\right)\right) \quad (26)$$

Therefore, for small probability values $\mathcal{P}_{T_\eta}(\eta)$, we can remove noise by thresholding out values below T_η. To choose a value for $\mathcal{P}_{T_\eta}(\eta)$, consider the non-trivial case of inequality (26), ie. when:

$$\frac{\sqrt{2\pi}\mathcal{P}_{T_\eta}(\eta)}{\sigma_\eta} + exp\left(\frac{-1}{2\sigma_\eta^2}\right) < 1 \quad (27)$$

Or:

$$\mathcal{P}_{T_\eta}(\eta) < \frac{\sigma_\eta}{\sqrt{2\pi}} \left(1 - exp\left(\frac{-1}{2\sigma_\eta^2}\right)\right) \quad (28)$$

Therefore, the upper bound of $\mathcal{P}_{T_\eta}(\eta)$ is found by substituting the upper bound of the noise variance in (28). It is obvious that the right hand side of the above inequality is always in $[0,1]$.

4 Experimental Results

In order to verify experimentally the algorithm, some artifitially shifted images were generated using the following model:

$$f_i = h \oplus I_i \quad i = \text{frame number} \tag{29}$$

where I_i is a high resolution image shifted by different values, h is a blurring kernel and $\oplus$ denotes the convolution. h has been introduced to demonstrate the possibility of taking into account the point spread function of the imaging system.

Therefore, each frame f_i is obtained by shifting a high resolution image followed by convolution and downsampling. The rate of downsampling along each dimension is larger than the shift values so that the resulting downsampled images contain subpixel shifts. Note that, no knowledge of the blurring kernel is required for the registration. The only assumption made on h is that its response is invariant from one frame to another.

The algorithm was tested on several images of different nature. Figure 3. shows an example of two aerial images with subpixel shifts between them. Figure 3 (c) and (d) show their cross power spectrum in the spatial domain prior and after removal of noise. Note that, due to the subpixel nature of the correspondence, there is no single coherent peak (as was the case for integer displacements). Instead, the signal power is distributed in the form of polyphase components of a 2D sinc function centered at the point of correspondence. This has been shown, more prominently, in Figure 3 (e), where a zoom in the area $[-3, 3] \times [-3, 3]$ of Figure 4 (d) has been displayed (recall that negative pixel values are due to periodicity).

Since the amplitude of a sinc function reduces rapidly as we part from its centre, it is obvious that some terms have been thresholded out as their amplitudes could not be distinguished with that of noise. However, due to the large value of SNR the majority of the signal power is recovered with no difficulty, around the peak point of the sinc function and its adjacent sidelobes (ie. at the points where the subpixel shifts are calculated).

In Figure 4, some of the images to which the algorithm was applied has been shown. The algorithm was also tested on many other images including indoor and outdoor robotic environments, with some of the results summarized in Table 1. We have also tested the method on many images with different dynamic ranges and artificially modified RGB combinations. These tests verify the independency of the algorithm from spectral modulus (ie. phase corrrelation only). Results on the SPOT image, for instance, are shown in Figure 5 and table 2.
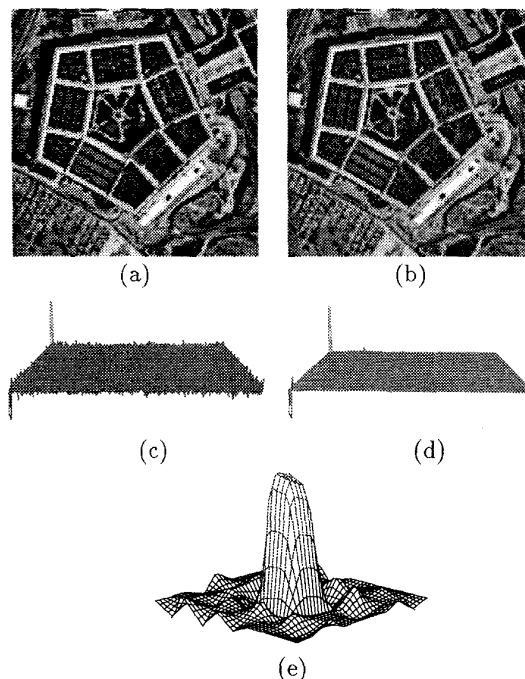

Figure 3: (a) & (b) aerial images with subpixel displacements, (c) & (d) cross power spectra before and after noise removal (spatial domain), (e) a zoom in the area where the signal power is mostly concentrated in figure 3(d)
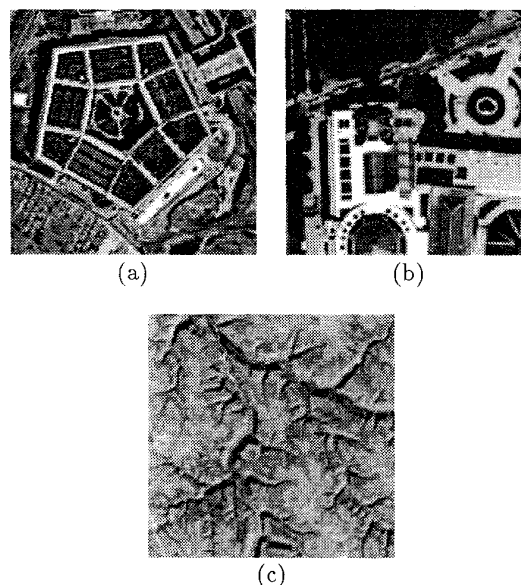

Figure 4: Some of the images uesed for experimentation: (a) & (b), aerial images of Pentagon and Paris, (c) a SPOT satellite image

Image	$(\Delta x, \Delta y)$	Estimates
Pentagon	(0.50, -0.50) (0.25, 0.50) (-0.25, -0.50) (0.0, 0.75)	(0.48, -0.51) (0.28, 0.49) (-0.25, -0.52) (0.0, 0.80)
Paris	(0.167, -0.5) (0.67, 0.25) (-0.33, -0.167) (0.33, 0.33)	(0.152, -0.49) (0.69, 0.33) (-0.32, -0.15) (0.325, 0.32)
SPOT	(0.83, 0.25) (0.33, -0.50) (-0.83, 0.167) (0.25, 0.33)	(0.84, 0.28) (0.34, -0.52) (-0.83, 0.151) (0.30, 0.33)

Table 1: Table of results for images in figure 4

(a)   (b)
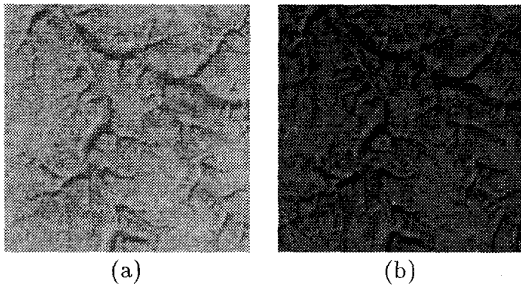
Figure 5: (a) & (b) two satellite images with modified dynamic ranges and RGB combinations

Image	$(\Delta x, \Delta y)$	Estimates
SPOT	(0.83, 0.25) (0.33, -0.50) (-0.83, 0.167) (0.25, 0.33)	(0.83, 0.30) (0.34, -0.53) (-0.84, 0.15) (0.29, 0.34)

Table 2: Table of results for images with different dynamic ranges and RGB combinations

5 Conclusion

A method of determining subpixel shifts has been proposed, herein, which does not resort to interpolation. The method is based on the phase correlation, and is proved to be very robust to correlated noise and luminance variations. Note that, methods that rely on interpolation would require an interpolation by a factor of 100, if one needs, for example, an accuracy of up to 2 significant figures. Results would, obviously, highly depend on the interpolation method.

Although, our analyses seem to be elaborated, the algorithm is hardly more complicated than the phase correlation method. The only overhead computations are noise removal and the calculation of the shifts $(\Delta x, \Delta y)$, which are trivial. Therefore, the speed of the algorithm, mainly depends on the Fourier transform, for which we have employed the FFT algorithm.

The accuracy of the results, depends on the noise variance, or more precisely on the signal to noise ratio. In other words, we would expect less accurate results

as we approach the lower limit of the signal to noise ratio. We will investigate this issue in future work.

References

[1] A. N. Akansu and R. A. Haddad. *Multiresolution Signal Decomposition.* Academic Press Inc., 1995.

[2] C. A. Bernstein, L. N. Kanal, D. Lavin, and E. C. Olson. A geometric approach to subpixel registration accuracy. *CVGIP*, 40:334–360, 1987.

[3] M. Berthod, H. Shekarforoush, M. Werman, and J. Zerubia. Reconstruction of high resolution 3d visual information. In *Proc. CVPR*, pages 654–657, Seattle, 1994.

[4] V. N. Dvorchenko. Bounds on (deterministic) correlation functions with applications to registration. *IEEE Trans. PAMI*, 5(2):206–213, 1983.

[5] T. S. Huang, editor. *Image Sequence Processing and Dynamic Scene Analysis.* Springer-Verlag, 1982. Nato Advanced Study Institute.

[6] T. S. Huang and R. Y. Tsai. *Image Sequence Analysis:Motion Estimation*, chapter 1, pages 1–18. Springer-Verlag, 1981.

[7] M. Irani and S. Peleg. Improving resolution by image registration. *Graphical Models and Image Processing*, 53(3):231–239, May 1991.

[8] D. Keren, S. Peleg, and R. Brada. Image sequence enhancement using sub-pixel displacement. In *Proc. CVPR*, pages 742–746, Ann Arbor, 1988.

[9] S. P. Kim and Wen-Yu Su. Subpixel accuracy image registration by spectrum cancellation. In *Proc. ICASSP*, pages 153–156, 1993.

[10] C. D. Kuglin and D. C. Hines. The phase correlation image alignment method. In *Proc. Int. Conf. on Cybernetics and Society*, pages 163–165, 1975.

[11] A. Papoulis. *Signal Analysis.* McGraw-Hill Book Company, 1977.

[12] H. Shekarforoush, M. Berthod, and J. Zerubia. 3d super-resolution using generalized sampling expansion. In *ICIP*, Washington DC, 1995.

[13] H. Shekarforoush, M. Berthod, and J. Zerubia. Sub-pixel reconstruction of a variable albedo lambertian surface. In *BMVC*, pages 307–316, 1995.

[14] H. Shekarforoush, M. Berthod, J. Zerubia, and M. Werman. Sub-pixel bayesian estimation of albedo and height. *International Journal of Computer Vision*, to appear.

[15] Qi Tian and M. N. Huhns. Algorithms for subpixel registration. *CVGIP*, 35:220–223, 1986.

[16] R. Tsai and T. Huang. Multiframe image restoration and registration. *ACVIP*, 1, 1984.

[17] M. Vetterli and J. Kovacevic. *Wavelets and Subband Coding.* Prentice Hall, 1995.